Probing water uptake gradient in an epoxy matrix via scanning electrochemical microscopy

Alexis Renaud, Florian Hache, Y. Elkebir, Julien Valette, Stéphanie Mallarino, Dao Trinh, Sébastien Touzain

Probing water uptake gradient in an epoxy matrix via scanning electrochemical microscopy

A. Renaud[1], F. Hache[2], Y. Elkebir[1], J. Valette[3], S. Mallarino[1], D. Trinh[1], S. Touzain[1]

1 : Laboratoire des Sciences de l'Ingénieur pour l'Environnement (LaSIE) UMR CNRS 7356, Université de La Rochelle, Pôle Sciences et Technologie, Avenue Michel Crépeau, 17042 La Rochelle Cedex 1, France

quang-dao.trinh@univ-lr.fr

2 : Institut Ingénierie Mécanique (I2M), CNRS Université de Bordeaux, 15 rue de Naudet, 33170 Gradignan, France

3 : TENSYL, 48 rue Jacques de Vaucanson, Pôle Arts et Métiers, 17180 Périgny, France

Abstract

Scanning electrochemical microscopy (SECM) is used to detect and observe the presence of water inside polymeric film at the microscopic scale around 200-500 µm. The principle is based on the use of SECM performed with a room temperature ionic liquid (RTIL) and $K_4Fe(CN)_6$ as redox sensor. The particular electrochemical behaviors obtained in such medium have been investigated by performing cyclic voltammetry and approach curves in negative feedback mode. Then, the cross-section of epoxy resin films has been repeatedly scanned using the SECM probe over several days of immersion in the RTIL. As the presence of water impacts the electrolyte viscosity, the electrochemical signal was sensitive to the amount of water around the microelectrode. The sensitivity of this technique to the presence of water released from the materials at the microscopic scale was demonstrated by comparing electrochemical signals obtained on dry and saturated specimens. Such results appeared to be very promising for the development of new methods to locally detect the presence of water in thick polymeric materials and to measure humidity gradient within the material thickness.

Keywords

Room temperature ionic liquids (RTIL); Scanning electrochemical microscopy; SECM; Water detection; Epoxy resin

1. Introduction

Among the various environments to which human technologies can be exposed, immersion in fresh water is one of the harshest conditions. In particular, metallic components can be subjected to strong corrosion phenomena and then lead to the failure of structural parts [1–3]. For this reason, polymeric materials are often preferred for immersed applications and are widely used in marine and submarine environments [4–6]. Parts can be made of pure polymeric materials (thermoplastic or thermoset matrixes) or various composite structures, such as glass fiber reinforced polymers (GFRP) or carbon fiber reinforced polymers (CFRP) [7–9]. Even though these lasts are not subjected to corrosion processes, they can still interact with the surrounding aqueous environment [10–12]. In particular, water molecules can penetrate and diffuse to the bulk of the immersed parts. The amount of absorbed water and the kinetics of the water ingress strongly depend on the chemical nature of the polymeric matrix [13]. Other internal parameters (manufacturing process, microstructure) or external parameters (temperature and composition of the aqueous environment) can also impact the quantity of water at the equilibrium and the speed of the water penetration [14].

In the case of thin polymeric systems, such as layers or membranes, the water saturation state is quickly reached and the specimens behave as homogeneous hydrated materials [15]. However, thicker parts need much more time to attain equilibrium [16], leading to the presence of a long-term humidity gradient through the thickness of the specimens. For instance, blades of industrial turbines are usually made of sandwich composites with glass/epoxy skins whose thickness vary from few millimeters at the tip up to few centimeters at the base. Thus, the time needed to reach a homogeneous water saturation state can be very long and the parts can present humidity gradients for the major part of their service life. Obviously, such gradients induce a heterogeneous distribution of properties (mechanical, dielectric, etc.) through the thickness of the materials. In such case, the modeling and the prediction of the macroscopic behavior of the whole parts becomes imprecise and much more complex. Being able to access the humidity gradient through a specimen is then a key step in predicting and understanding its global properties. Indeed, the durability of those blades is critical for the expected turbine life of 10 to 20 years. The prediction of the humidity profile, of the fatigue state and of the coupling of these processes is a primary interest. Therefore, the evaluation of the water distribution through the laminates has to be addressed.

Even though diffusion laws such as Fick [17,18] or Langmuir equations [19,20] are very useful for the prediction of water concentration in a material, it becomes more difficult to use them for heterogeneous materials or structures with complex geometries. If the diffusion parameters

describing the water uptake kinetics and equilibrium are not well known and characterized, the challenge gets even bigger. A large number of studies deal with the estimation and the prediction of such profiles [21–25].

If one wishes to know the distribution of water involved in a solid material, IR and Raman microscopes give precise information in a short time. The concentration of water vapor can be detected by the optical hygrometer measurement. The first known measurements of the water vapor absorption in the infrared (IR) were performed by Fowle (1912) [26]. There are some important requirements for the selected wavelength: minimize the collision broadening with the other components, high selectivity with regard to water, and high contrast in optical properties between water and other components of the material [27].

There are some drawbacks when using the IR, or Raman microscopies to evaluate the water content in epoxy resin. Andrey E. Krauklis et al. [28] used the Fourier transform near-infrared (FT-NIR) spectroscopy to measure the water content of amine-epoxy neat resin and Fiber-Reinforced Composites. Based on the physics of Beer–Lambert law, this method can be used to a wide range of samples, including thin ones. However, it is important to keep in mind that this approach has some drawbacks. As an example, monitoring of carbon fiber-composite materials is likely to be limited if the sample is too thick or non-transparent within the researched radiation wavelength range. Other spectroscopic approaches include Raman, which is less sensitive to water than FTIR, and reflectance FTIR, which primarily provides information on the material's surface. The weak sensitivity of water detection is a downside of Raman spectroscopy. The conversion efficiency of the Raman effect is low because only a small fraction (approximately 10^{-6}) of the original photons are non-elastically dispersed [29].

C. Marro Bellot et al. [30] have embedded evanescent optical fiber sensors at different depths of a composite material to detect the moisture diffusion through the thickness of the epoxy samples. Eight sensors were used at depths ranging from 0.8 to 2.3 mm. Since the number of the sensors are limited, the resolution of this method is weak and not applicable to study the water profile of a thin epoxy resin (thickness around 400 μm).

The SECM technique could be fruitful to measure the moisture profile of the epoxy material. Using the electrochemical scanning tip with a diameter of 10 μm, water molecules can be locally detected by the current of the tip so the humidity profile can be estimated. Instead of using several embedded sensors, this method relies on the electrochemical scanning tip, which can measure smaller dimension, with a higher scanning resolution. This method can also be applied to a transparent or non-transparent sample because the measured signal is the electrochemical current.

This work focuses on the detection of the water profile across the material thickness by using scanning electrochemical microscopy (SECM) experiments performed in a dry room temperature ionic liquid (RTIL). After a theoretical justification of the proposed methodology, the experimental protocol is detailed and first results are presented, validating the consistency of the method.

2. Principle

2.1. Detection of humidity in RTILs using electrochemistry

The SECM technique has already been used on polymeric materials in order to investigate various phenomena such as dimensional swelling [31], physical aging [32] or internal stress [33]. In these studies, electrochemical measurements have been performed in aqueous electrolytes [34,35] in order to perform an in-situ monitoring of the swelling when the specimens were exposed to water.

In the case of the present work, the approach is quite different. Naturally, trying to detect the presence of water via an aqueous media would be a nonsense. Nevertheless, electrochemistry can also be performed in several non-aqueous electrolytes. For instance, RTIL have been widely developed in the past years to perform original electrochemical reactions [36–40]. Nkuku et al. [41] have demonstrated the feasibility of performing SECM with ferrocene dissolved in non-aqueous solvent (deep eutectic solvent). However, the high viscosity of the solvent leads to specific behaviors due to convection and diffusion mixed regimes. In such a high viscous solvent, the diffusion coefficient of redox species in RTIL are a hundred times lower than those in aqueous media [42]. RTILs can also be used to analyze the inward and outward electrolyte diffusion processes (in dry conditions) in epoxy coatings [43].

In the presented method, a water-free RTIL is used as electrolyte in order to detect water molecules coming from a wet thermoset material sample. Indeed, the impact of the presence of water on electrochemical signals obtained in RTILs has already been demonstrated by different authors. Two main cases can be distinguished.

Redox activity provided by water molecules: Zhao et al. [44] performed voltammetry experiments using a gold electrode in two aprotic RTILs containing different amounts of humidity. Water molecules are involved in the following reactions (Eqs. (1) and (2)):

$$Au + H_2O \rightarrow AuO + 2H^+ + 2e^- \quad (1)$$

$$2AuO + H_2O \rightarrow Au_2O_3 + 2H^+ + 2e^- \quad (2)$$

The voltammetry signal, and more specifically the current peak associated with Eq. (1), is significantly impacted by the amount of water present in both tested RTILs. The authors also demonstrated the linear relation between the water concentration in the RTILs and the current peak value.

Redox activity provided by an additional compound: Qian et al. [45] performed cyclic voltammetry and square wave voltammetry in RTILs using potassium ferricyanide as the redox specie. Even though water is not involved in the electrochemical reactions observed by voltammetry, a linear relationship between the amount of water in the RTILs and the anodic peak current measured in square wave voltammetry has also been emphasized. The linearity has been observed in both hydrophilic and hydrophobic RTILs. The authors demonstrated that the dependence between the water concentration and the anodic peak current in the bulk solution can be attributed to the impact of water molecules on the viscosity of the RTIL and then on the diffusion coefficient of the redox specie. Indeed, the anodic peak current value of a macroscopic electrode can be approximated by the Randles-Sevcik equation (eq 3) [46]:

$$i_{peak} = 0.446nFAC_0\left(\frac{NF}{RT}\right)^{1/2} v^{1/2}D \qquad (3)$$

where n is the number of electrons transferred per molecule, F the Faraday constant, A the area of the electrode, C_0 the concentration of the redox probe, v the scan rate and D the diffusion coefficient. This diffusion coefficient of the redox species depends on the viscosity of the RTIL, which is itself dependent on the presence of water molecules. It is worth to mentioning that Qian et al. [47] also checked that the presence of potassium ferricyanide does not affect the diffusion of water in the RTILs.

2.2. Electrochemistry in RTILs brought to the microscopic scale

The tight relation between the amount of water in a RTIL and the electrochemical response has been demonstrated on macroscopic electrodes. The purpose of the present work is to apply this principle at the local microscopic scale, using a microelectrode. The SECM technique has been greatly developed in the past decades and finds relevant applications in a broad range of research fields [31,48–51]. This scanning technique allows investigating local electrochemical reactions at the microscopic scale. In this paper, SECM is performed in a RTIL using the principle previously detailed in order to locally assess the presence of water. This approach takes advantage of i) the low diffusivity of water molecules in the RTIL, ii) the RTIL hydrophilicity to force the water to get out of the material, iii) the water-free environment that prevents to have experimental artifacts and iiii) the use of

157 microelectrodes to measure the local concentration of the redox mediator close to the polymeric
158 material.

159 Figure 1 illustrates the developed protocol. A microelectrode (10 µm diameter) is used as the SECM
160 tip. The SECM tip is scanned over the polymeric material, with a constant tip-to-sample distance of 5
161 µm. The polymeric material plate, that was previously immersed in water, presents a humidity
162 gradient through its thickness. Depending on the hydrophilicity of the RTIL and on its viscosity, water
163 molecules will progressively come out of the polymeric material and diffuse within the RTIL, locally
164 modifying the electrochemical properties of the electrolyte, especially the current intensity. The
165 variations of the electrochemical signal over a scan line can then be attributed to the local
166 concentration of water in the RTIL, which is itself depending on the local amount of water in the
167 material. Obviously, electrochemical variations will be more representative of the humidity gradient
168 as the microelectrode is brought as close as possible to the specimen surface.

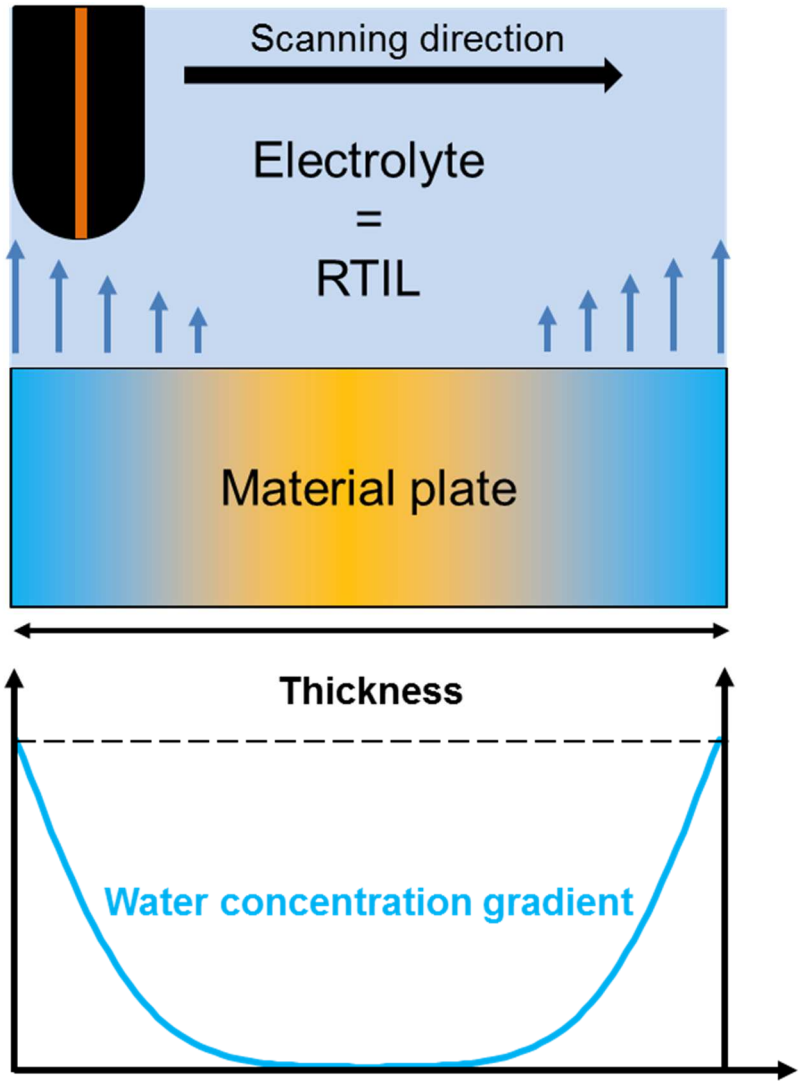

169

Fig. 1: principle of the local detection of water molecules coming out of a wet specimen with a water concentration gradient through its thickness

To electrochemically detect water molecules, potassium ferricyanide $K_4Fe(CN)_6$ has been used as the redox mediator. Because the electrochemical process in this approach does not include water, no water is produced or consumed during the measurement, which eliminates the possibility of artefacts. The choice of the RTIL has been done according to two criteria: hydrophilicity in order to promote the desorption of water from the specimen, and high viscosity in order to have a slow diffusion of water in the RTIL and offer enough time for measurement. For these reasons, 1-butyl-1-methylpyrrolidinium triflate has been selected.

As mentioned hereinbefore, due to the high viscosity of RTIL, one should consider the mixed convection-diffusion regime. This term can be characterized by the Peclet number (*Pe*) [52,53]:

$$Pe = \frac{v_{tip}\, a}{D} \qquad (4)$$

where v_{tip} the tip velocity, a the tip radius, and D the diffusion coefficient.

Moreover, potential unexpected interactions between this RTIL and the resin samples have been previously checked by immersing dry epoxy specimens in the RTIL, for 5 days. No mass variations and no dimensional changes have been observed, attesting the absence of swelling and/or degradation mechanisms when the polymeric materials are exposed to such electrolytes.

3. Sample preparation

3.1. Specimens

To validate the protocol, samples of epoxy resin have been prepared. They were obtained by mixing an epoxy precursor (diglycidylether of bisphenol A or DGEBA, Sigma Aldrich, ref. 1675-54-3) with an amine hardener (Jeffamine 230, Sigma Aldrich, ref. 9046-10-0).

Both components have been mixed using a mechanical mixer for 10 minutes and up to 2500 rpm. The mixture is then degassed for 20 min at room temperature to remove any air bubbles. The resin is then spread between two aluminum plates covered with a sheet of Teflon and spaced by spacers in order to control the thickness of the films (thickness 200 - 500 µm) and cured at 120 °C for 14 hours [54]. Such low thicknesses have been chosen in order to obtain samples that can be quickly saturated with water.

3.2. Conditioning

After elaboration, samples have been dried for at least one week under vacuum in a desiccator to remove any potential water present in the films.

To emphasize the ability of the method to locally detect water from a wet material, dry samples have been compared with saturated ones. To reach water saturation, resin specimens have been immersed in distilled water at 35 °C for 5 days and frequently weighted until the water uptake reaches its saturation value of about 3 % in weight.

3.3. Testing protocol

As the sample has to be fixed during the experiment, a sample holder made of PU resin and PTFE has been built and used after drying, as presented on figure 2. The scanned surface should be as flat as possible in order to avoid topographic artefacts. This means that the sample surface has to be cut and equalized with the surface of the PU and PTFE materials from the sample holder. However, polishing is excluded, with or without water. Indeed, wet polishing would bring unexpected water to the system, and dry polishing would increase the temperature of the sample surface due to friction and induce desorption of water molecules. For the same reason, the duration of the preparation of the sample system should be as short as possible in order to limit water desorption before the analysis.

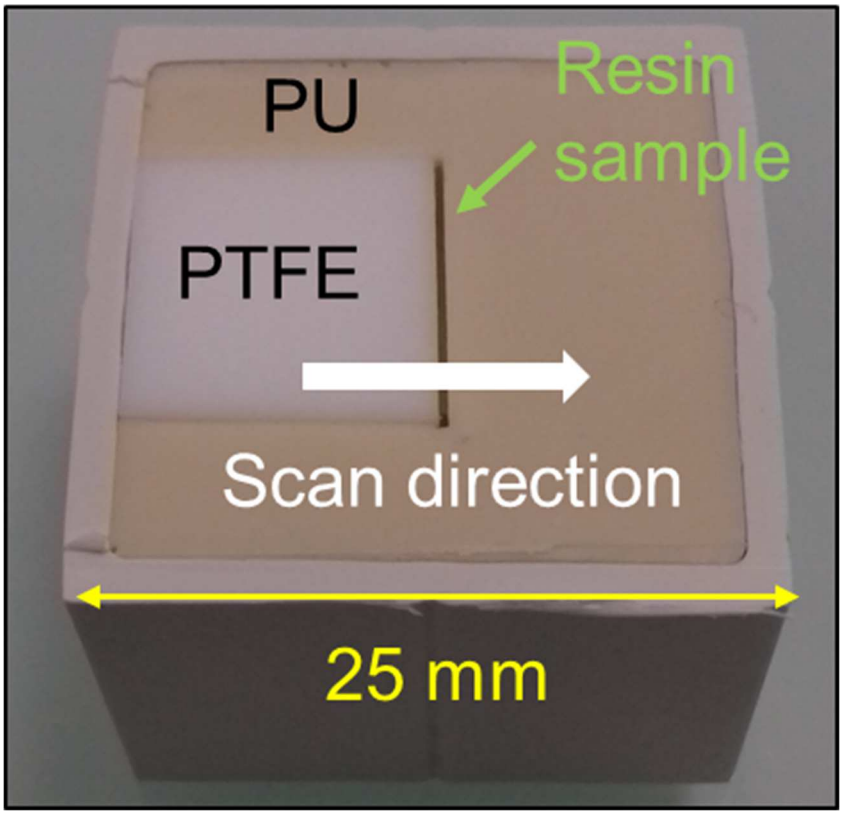

Fig. 2: sample holding system

After extraction from the desiccator or from the immersion bath, resin samples have been directly clamped into the sample holder and the surface has been cut using a microtome knife equipment model HM 340E from Microm Microtech, offering a fast, dry and room temperature cutting process. The sample holding system has then been inserted in the electrochemical cell (figure 3) and the RTIL has been poured to start the experiment. Finally, in order to prevent water ingress from the air, a thin layer of liquid silicon oil has been deposited on top of the RTIL liquid. The proposed setup ensures that the local variations of the electrochemical signal are only attributed to the water coming from the resin sample.

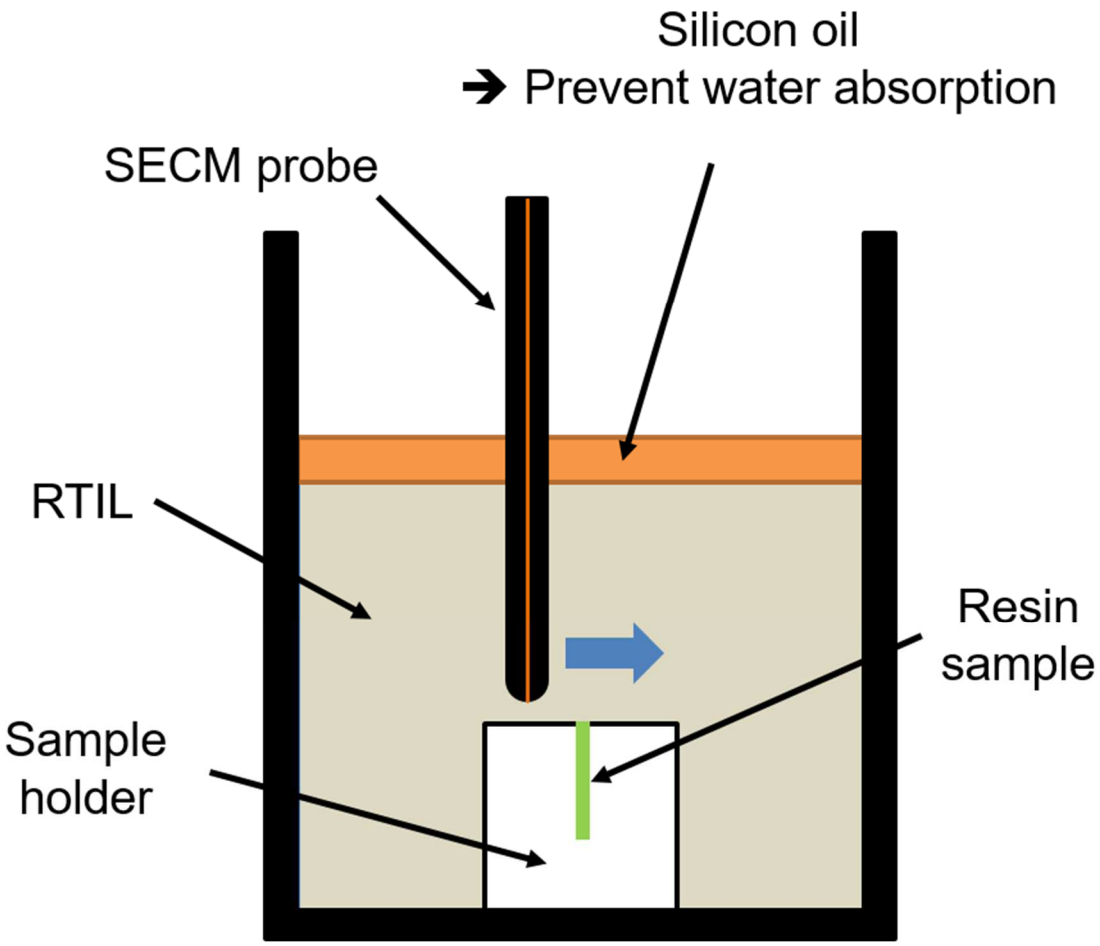

Fig. 3: Experimental setup during the electrochemical tests

The settings of the experiment have been optimized based on the preliminary electrochemical investigation, in order to guarantee a good compromise between the resolution of the characterization and the acquisition of a sufficiently high electrochemical current approach curves. A distance of 5 µm between the microelectrode and the sample has been chosen based on approach curves.

4. Experimental setup

SECM measurements have been performed using a SECM M470 equipment from Biologic, equipped with a platinum microelectrode with a diameter of 10 µm. The counter electrode, which also stands as a pseudo-reference, was a platinum wire dipped into the RTIL. The temperature was controlled by a thermostat cell at 25 °C.

Potassium ferricyanide $K_4Fe(CN)_6$ was added to the RTIL in order to get a 10 mM concentration and to provide the redox activity. In order to remove any trace of water, the RTIL solution has been dried at 60 °C for at least 90 minutes under vacuum in a desiccator [55]. Then, after cooling down to 25 °C, the electrolyte was poured at the very last minute before the beginning of the experiments.

Cyclic voltammetry has been performed using this setup in order to verify the electrochemical processes occurring at the microelectrode in the RTIL. Figures 4.a and 4.b present the obtained voltammogram of the $K_4Fe(CN)_6$ dissolved in water and in RTIL, respectively.

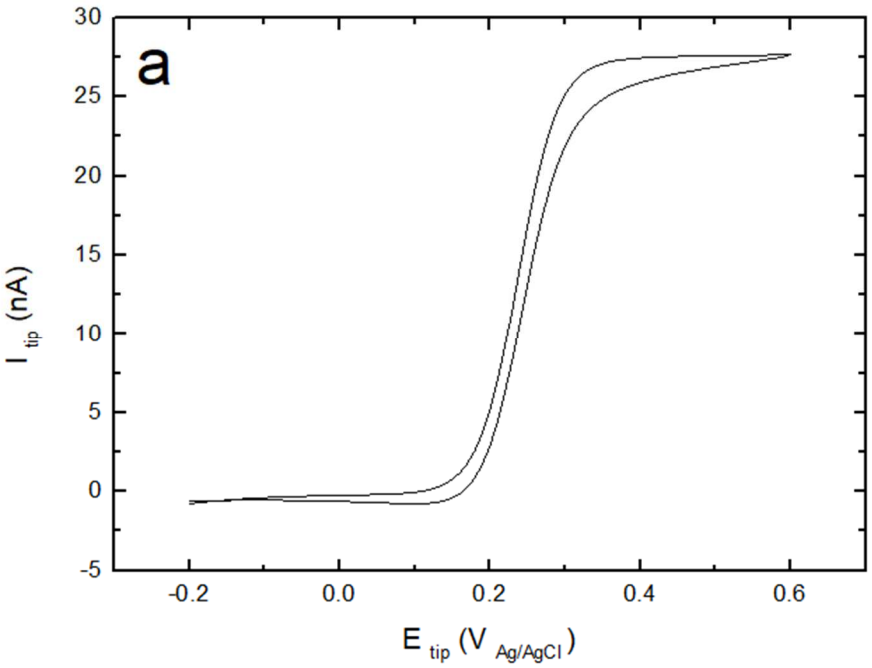

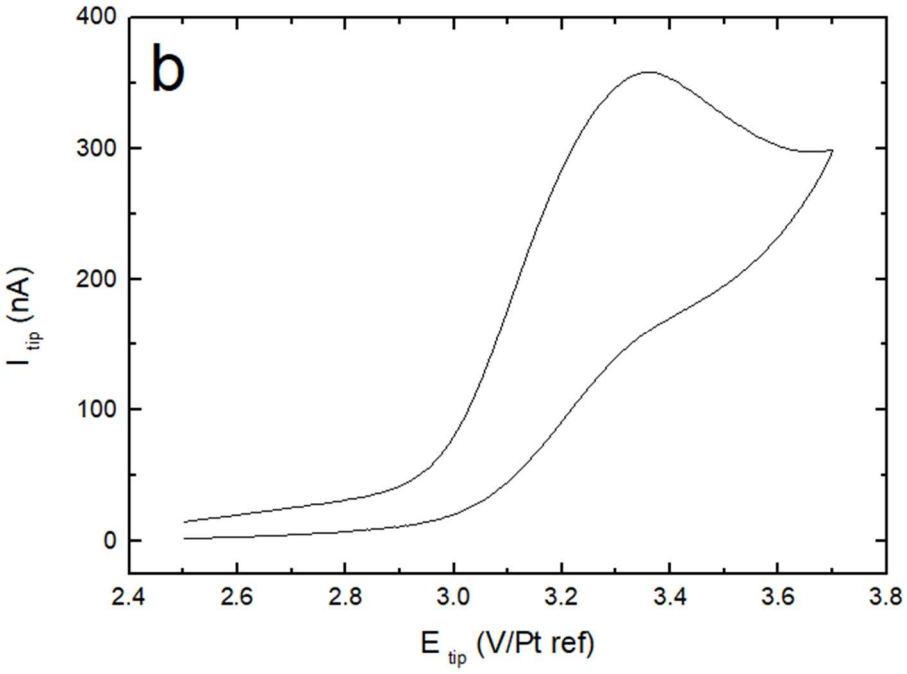

Fig. 4: Cyclic voltammogram (sweep rate 20 mV/s) obtained a) in water, and b) in RTIL for the $[Fe(CN)_6]^{3-}/[Fe(CN)_6]^{4-}$ couple

In these conditions (RTIL + pseudo-reference), the standard potential of the redox couple was estimated to be approximately $E_0(Fe(CN)_6]^{3-}/[Fe(CN)_6]^{4-}) = 3.25$ V/Pt ref. As mentioned previously, at the same sweep rate, it is more difficult to obtain the steady state voltammogram at the microelectrode in RTIL compared to water because of the very slow diffusion of redox species in the RTIL. Figure 4b shows the non-steady-state behavior of the microelectrode in a high viscous environment. This behavior has been confirmed by the study of the effect of viscosity on steady-state voltammetry of the SECM microelectrode by Kevin R. J. Lovelock et al [56].

Figure 5 presents the normalized approach curves in the RTIL for 3 approaching speeds v = 1; 2; and 5 µm/s, respectively. It should be noted that 1 µm/s is the lowest scan speed allowed by the setup. By approaching the tip to the insulating material, negative feedback approach curves could be observed. However, when the tip approaches near the surface (L = 0.5), the tip current increases. The shape of such approach curves can be surprising compared to what is usually obtained in aqueous electrolytes. Due to the high viscosity of RTIL, the moving microelectrode can induce forced convection phenomena. Forced convection contributes to the additional flux to the tip, thereby increases the tip current. This behavior has been observed and explained by C.A. Nkuku et al [32].

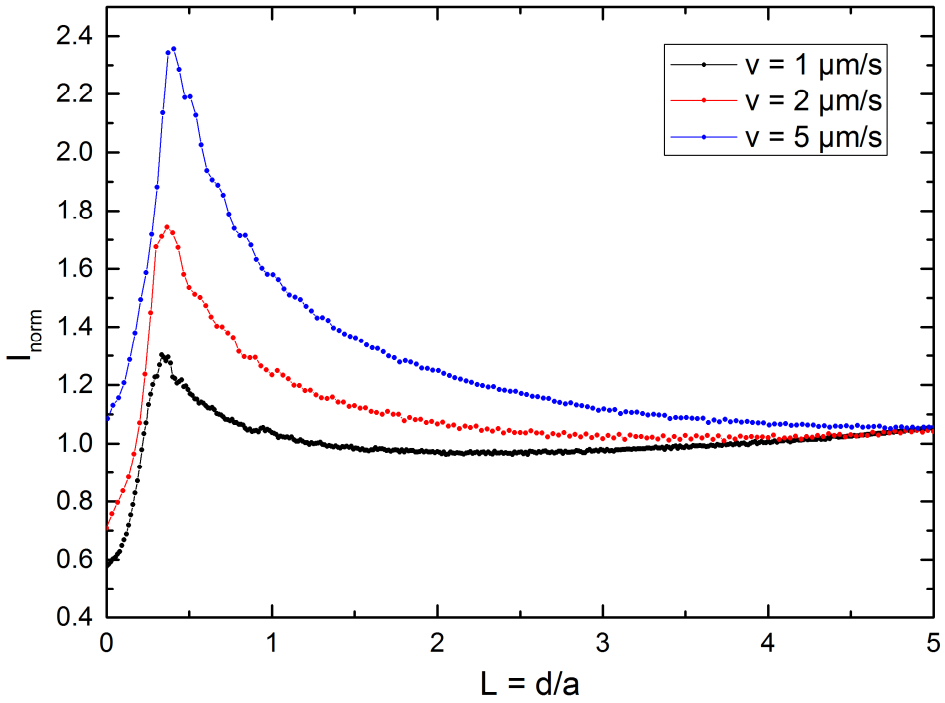

Fig. 5: Normalized approach curves obtained in RTIL for different speed values.

In particular, the current peak occurring as the tip reaches the surface is specific to viscous media. This phenomenon has been well described and explained by Nuku et al. [53], linking it with convection processes at the neighborhood of the surface. The amplitude of this current peak is directly related to the speed of the microelectrode, as shown on figure 5. This unusual behavior is also observed in other high viscosity RTILs [57].

The Peclet number (Pe) depends on the tip velocity, electrode radius and diffusion coefficient (see eq. 4). For example, in water, the typical *Pe* value is 0.03 (with a = 10 µm, D = 7×10^{-10} m^2/s, v = 2 µm/s), but in this RTIL, *Pe* is much higher and equal to 4.44 (with a = 10 µm, D = 4.5×10^{-12} m^2/s, v = 2 µm/s). In both cases, the speed values and the tip radius are the same, only the diffusion coefficient of the redox mediator D changes. Choosing the very slow tip velocity can reduce the *Pe* value. It can be observed that this current peak is obtained for all the tested speed values. As 1 µm/s is the lowest approaching speed available on the equipment, this unusual behavior cannot be avoided with the experimental setup used in this work.

The approach curves (Fig. 5) present a current plateau far from the surface, and a sharp current drop as the microelectrode arrives on the surface, which is typical for an approach curve performed on an insulating material. Indeed, the proximity between the sample surface and the microelectrode blocks

the arrival of redox species, drastically diminishing the current value. Approach curves can then be used in the negative feedback mode to find the position of the specimen surface.

During this work, the approaching speed is fixed as 2 µm/s in all measurements (approach curves, and scan lines). This speed has been chosen as a compromise between the limitation of convection phenomena and the scan duration.

In order to get as close as possible to the surface of the specimens, approach curves have been performed to detect the position of the specimens. The tip is then retracted from the material surface of about 5 µm. Repeated scan lines have then been performed above the material surface at this same tip-to-substrate distance.

The SECM tip can be used to detect the amount of water released from the material. A simple test is made to verify this approach: a small amount of water is added in the ionic liquid, and the tip current is measured for each addition. At the end, 1 ml of water was added to 45 ml of ionic liquid, so the concentration is 0.025 ml of water per 1 ml of RTIL. Before measuring the tip current, the mixture is well homogenized for 5 minutes.

Figure 6 shows the cyclic voltammetry results during the addition of water. The tip current increases with the amount of water present in the RTIL because the diffusion coefficient increases as the volume of water in RTIL grows, as previously explained. This result demonstrates that this method may be used to detect and measure the humidity gradient emitted by an epoxy substance.

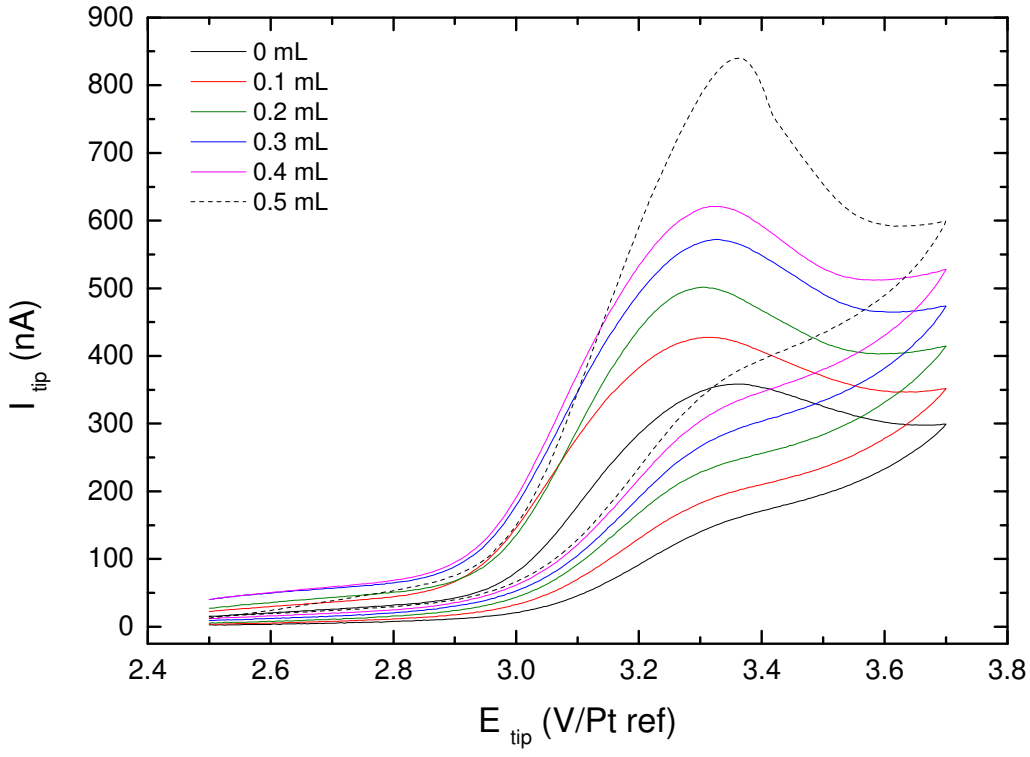

Fig. 6: Cyclic voltammetry of the tip obtained for different water volume added into the dry RTIL

A calibration curve can be used to quantify the water content released from the material. Figure 7 presents the calibration curve of the normalized current of the tip as a function of the humidity amount in the bulk solution (the ratio between the water volume added over the ionic liquid volume).

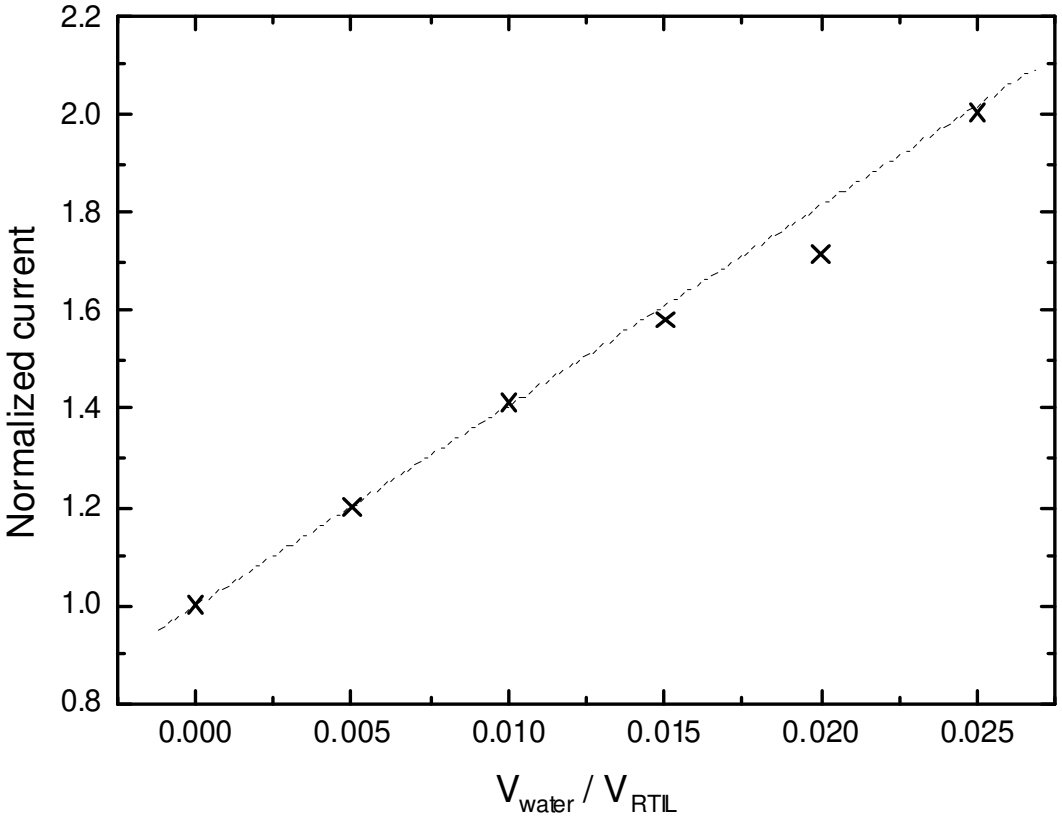

311

312 Fig. 7: The normalized current of the tip as a function of water content in the RTIL

313 The current of the tip is normalized with the quasi-steady state current, measured at 3.7 V/Pt ref. As
314 observed in Fig. 7, the tip current can be doubled with a very small amount of water added (2.5
315 vol.%). This method appears then very promising to quantify the humidity released from a material.
316 Since the amount of water detected close to the surface, and the amount of water diffused into the
317 bulk solution are different, the calibration curve as shown in Figure 7 can be used as a proof of
318 concept. To correlate the exact amount of water content released from the material, the exact tip-
319 substrate distance should be known to establish the calibration curve.

320 **5. Results**

321 **5.1. Scan over dry resin**

322 First, a dry resin specimen has been characterized in order to record a reference electrochemical
323 behavior, in the absence of any water.

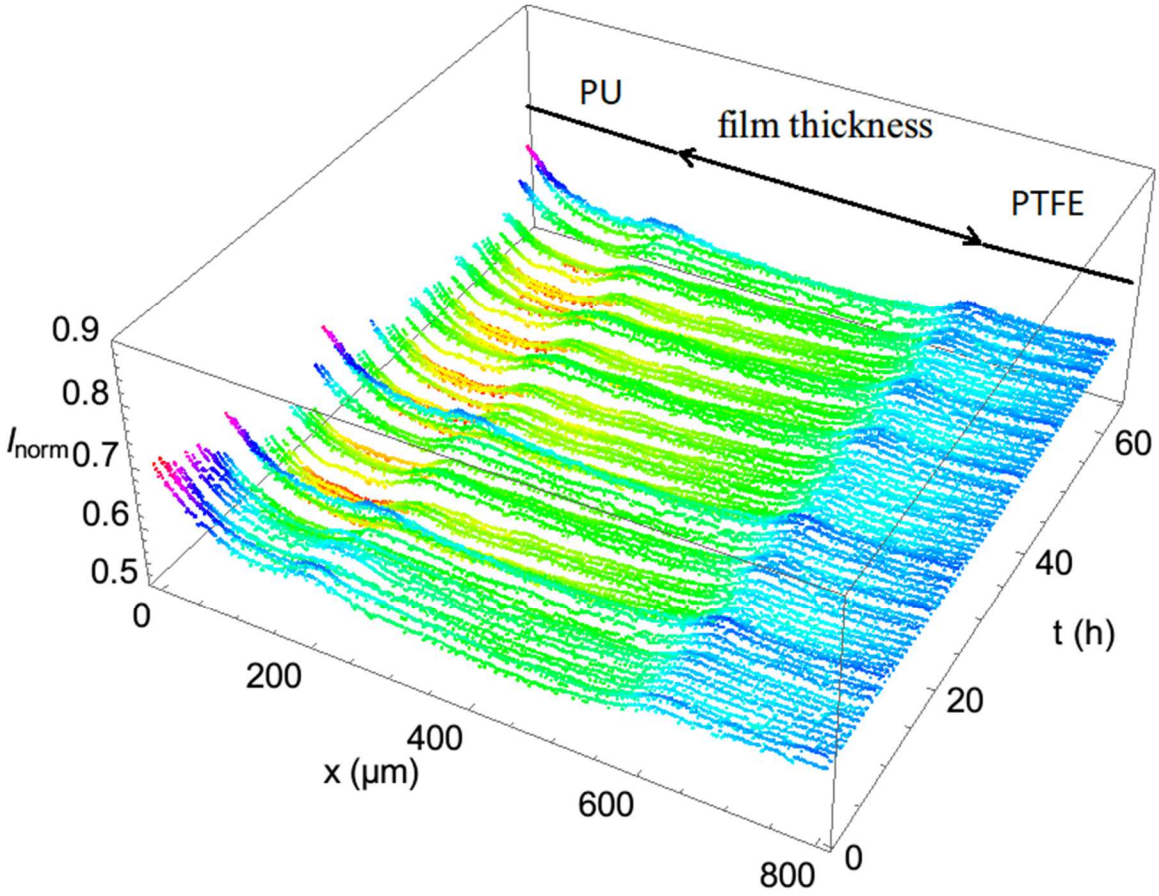

Fig. 8: The evolution of line scans over the dry film sample (400 µm thick) during 60 hours of RTIL immersion.

Figure 8 shows line scan obtained over the dry film during the 60 hours of immersion in the RTIL. The film position is shown with the arrow (thickness around 400 µm). The tip is moved from the left (x = 0 µm) to the right (x = 800 µm). From x = 0 µm to x = 200 µm, this is the PU part (see Fig. 2) from the sample holder and from x = 600 µm to x = 800 µm, this is the PTFE side.

At the beginning, the tip current is higher due to the initial convection of the tip. Therefore, the current is normalized with the quasi-steady state current when the tip is near the end of the scan (x = 800 µm). The center of the material is around the middle of the scan (x = 400 µm). The tip potential is kept at 3.7 V/Pt ref, the tip velocity 2 µm/s. Scans have then been repeated every 5 minutes for 60 hours.

The line scan over a 400 µm thick dry film didn't change during the time. It can be observed that the signal is almost completely flat all over the scan distance. As the thin film is completely dry, no water is detected over the sample thickness (from x = 200 µm to x = 600 µm). A slight slope is noticeable, attributed to the tilt of the sample surface. Such a tilt is not surprising considering the relatively big size of the characterized zone.

Only two small peaks can be observed. The distance between these two peaks corresponds to the thickness of the characterized sample. They can be attributed to topographic variations, easily explained by the non-ideal interface between the sample and the sample holder. The scan profile is stable over the whole period of characterization. Indeed, no evolution of the current is observed up to 60 hours. It is consistent with the absence of water and the characterization of a dry sample. It also attests that the setup is efficient to prevent the ingress of external water from the air.

5.2. Scan over water saturated resin

A water saturated resin specimen has been characterized in the same conditions in order to evaluate the ability of the method to detect the presence of water. Scans have been performed every 5 minutes for more than 90 hours. Figure 9 shows the scan signal obtained in these conditions for the saturated film sample. The film position is marked with the arrow.

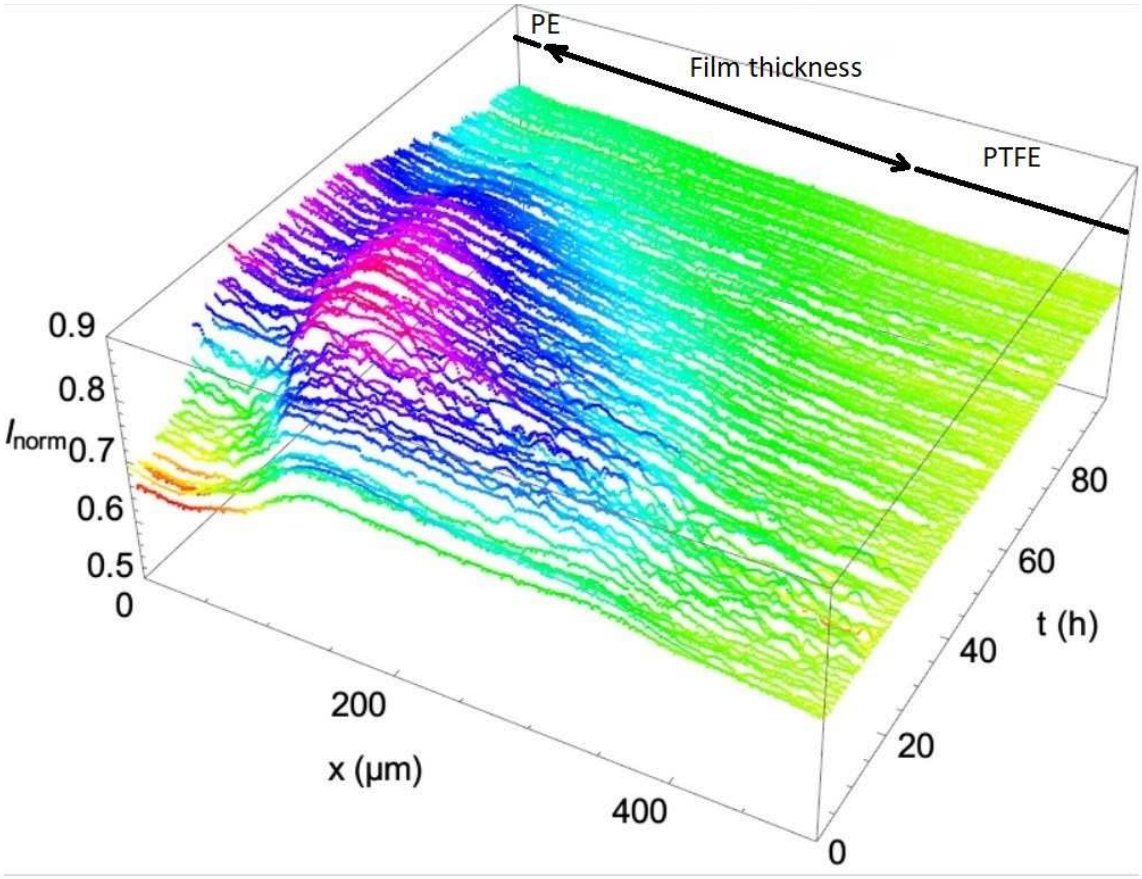

Fig. 9: The evolution of line scans over the saturated film sample (250 µm thick) over 4 days of RTIL immersion

The difference with the signal previously obtained on the dry sample is significant. The signal is not flat, as its value is higher over the resin material compared to the baseline. During the first 20 hours of immersion, the tip current over the wet sample surface increases from x = 150 µm to x = 400 µm, which corresponds to the film thickness. This increase is due to the release of water from the wet film to the RTIL environment. Indeed, the presence of water locally decreases the viscosity of the RTIL, increasing the tip current (due to enhanced diffusion coefficient of the redox specie). Though a symmetric profile could be expected, the topography and the tilt of the sample may have disturbed the ideal shape of the profile, resulting in slightly dissymmetric curves. Indeed, a slight tilt of the sample surface has to be considered, as well as for the dry sample presented above.

After 80 hours of immersion, the tip current above the sample has become flat. This can be interpreted as there is no more water released from the sample after a very long period of immersion. Compared to figure 8 for the dry film (at the same scale), a signal peak can be observed above the wet film.

5.3. Evolution of the current signal over time

The evolution of the current response over immersion time in the RTIL for dry and saturated specimens has been investigated. The variation with time of the normalized current measured in the center of the sample has been plotted, as shown on figure 10.

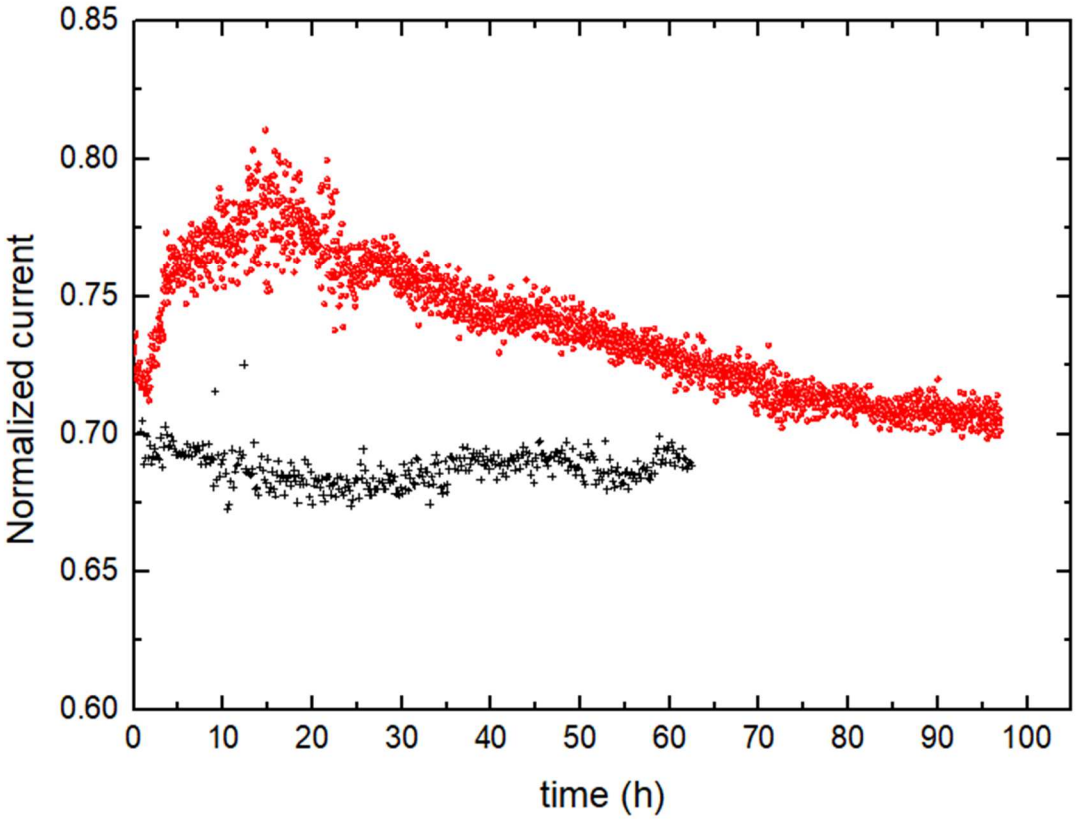

Fig. 10: Evolution of the normalized current in the center of the samples versus immersion time in RTIL (red: saturated film, black: dry film)

The difference is clear. The dry specimen confirms its stable behavior with a constant value of the normalized current all over the immersion period.

Comparatively, the normalized current measured for the saturated specimen significantly evolves. A sharp increase from 0.7 to approximately 0.8 is observed during the first 15 hours. Then, the normalized current value slowly decreases down back to a value of 0.7. Such an evolution can be explained and described as schematized in figure 11.

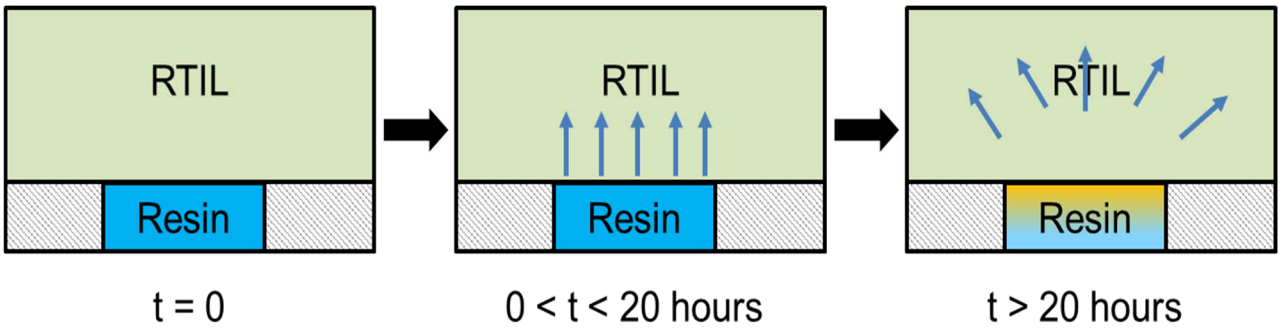

Fig. 11: Illustration of the different steps involved in the evolution of the current observed on the water saturated resin. Blue arrow: flux of desorbed water

At the beginning of the immersion in the RTIL, few water molecules had time to desorb and reach the neighborhood of the microelectrode, which is 5 µm away from the surface. As time goes by, water progressively desorbs and diffuses in the RTIL, increasing the tip current value. The maximum of the current value corresponds to the moment at which water has fully desorbed from the resin. From this point, water continues diffusing to the bulk of the RTIL, while no more water molecules are provided by the sample. Indeed, the diffusion of water molecule is faster in the RTIL than in the resin, inducing the progressive decrease of the normalized current value back to its initial value.

To evaluate the rate of water release, it is necessary to establish a calibration curve with the same operational condition (tip-to-substrate distance, temperature, the range of water content). Figure 10 can also be used to calculate the amount of water released by comparing the base line (for dry film resin) and the rate of water release as a function of time (red point for the saturated film). The profile of water released over the material surface can also be compared between the simulation obtained by COMSOL Multiphysics and the experimental result obtained by the SECM. These points are currently under investigation in our lab.

6. Conclusions

In this work, we proposed a new experimental protocol to evaluate the humidity profile in a polymeric material using SECM in RTIL medium. A sample preparation process has been proposed in order to keep the water concentration of the specimens as close as possible to its state before removal from immersion in water. In particular, the use of fast and room temperature processes for the sample preparation allows to preserve the water distribution in the samples.

Dry and saturated samples have been compared according to the proposed methodology. Obtained results emphasize the sensitivity of the SECM technique to the water concentration at the microscopic scale. From the evolution of the current signal over immersion time in the RTIL, it can be deduced that a window of approximately 20 hours is available for the characterization of the humidity profile. For longer periods of time, water molecules would no longer be released by the specimen and water will just diffuse to the bulk of the RTIL. The duration of this window would of course be influenced by the nature of the resin and of the RTIL. When working with high viscosity ionic liquid, slow scanning speed is required to reduce the velocity. This is the possible drawback of this approach when a large sample is scanned. The time required to perform the 2D scan with such a slow scanning speed could be too long.

The method provides a benefit over the conventional analysis providing the possibility to detect the water content over a thin epoxy resin surface. Based on a scanning electrochemical tip, the water content released from the sample surface can be estimated. The quantitative relation between the water content and the tip current was successfully established. Unlike optical measuring, which can only be used on transparent materials, this method can be applied to both transparent or non-transparent material. A good resolution of the humidity profile over a 400 µm film thickness has been also obtained.

Declarations

Funding

This work has been carried out in the frame of MEVEF R&D program lead by TENSYL, I2M and LaSIE laboratories funded by the Agence Nationale de la Recherche (ANR) (reference ANR-10-IEED-0006-23) and supported by Région Nouvelle Aquitaine.

Conflicts of interest

The Authors declare that there is no conflict of interest.

Availability of data and material

Not applicable

Code availability

Not applicable

References

[1] D. Andrade, M. Ros, S. Hor, Study of microbiologically induced corrosion of 5052 aluminum alloy by sulfate-reducing bacteria in seawater, Materials Chemistry and Physics. 241 (2020) 122296. https://doi.org/10.1016/j.matchemphys.2019.122296.

[2] Y. Gao, L. Ward, L. Fan, H. Li, Z. Liu, A study of the use of polyaspartic acid derivative composite for the corrosion inhibition of carbon steel in a seawater environment, Journal of Molecular Liquids. 294 (2019) 111634. https://doi.org/10.1016/j.molliq.2019.111634.

[3] A. Mostafanejad, M. Iranmanesh, A. Zarebidaki, An experimental study on stress corrosion behavior of A131 / A and A131 / AH32 low carbon steels in simulated seawater, Ocean Engineering. 188 (2019) 106204. https://doi.org/10.1016/j.oceaneng.2019.106204.

[4] A. Gagani, A. Krauklis, A.T. Echtermeyer, Anisotropic fluid diffusion in carbon fiber reinforced composite rods : Experimental, analytical and numerical study, Marine Structures. 59 (2018) 47–59. https://doi.org/10.1016/j.marstruc.2018.01.003.

[5] A.I. Gagani, A.T. Echtermeyer, Influence of delaminations on fluid diffusion in multidirectional composite laminates – Theory and experiments, International Journal of Solids and Structures. 0 (2018) 1–11. https://doi.org/10.1016/j.ijsolstr.2018.09.009.

[6] A. Siriruk, D. Penumadu, Degradation in fatigue behavior of carbon fiber-vinyl ester based composites due to sea environment, Composites Part B: Engineering. 61 (2014) 94–98. https://doi.org/10.1016/j.compositesb.2014.01.030.

[7] A. Kootsookos, A.P. Mouritz, Seawater durability of glass- and carbon-polymer composites, Composites Science and Technology. 64 (2004) 1503–1511. https://doi.org/10.1016/j.compscitech.2003.10.019.

[8] B. Sharma, R. Chhibber, R. Mehta, Seawater ageing of glass fiber reinforced epoxy nanocomposites based on silylated clays, Polymer Degradation and Stability. 147 (2018) 103–114. https://doi.org/10.1016/j.polymdegradstab.2017.11.017.

[9] P. Davies, P.Y. Le Gac, M. Le Gall, M. Arhant, Marine Ageing Behaviour of New Environmentally Friendly Composites, Solid Mechanics and Its Applications. 245 (2018) 225–237. https://doi.org/10.1007/978-3-319-65145-3_12.

[10] P. Davies, Y.D.S. Rajapakse Editors, Durability of Composites in a Marine Environment, n.d. https://doi.org/10.1007/978-94-007-7417-9.

[11] M. Landowski, M. Budzik, K. Imielinska, Water absorption and blistering of glass fibre-reinforced polymer marine laminates with nanoparticle-modified coatings, Journal of Composite Materials. 48 (2014) 2805–2813. https://doi.org/10.1177/0021998313503877.

[12] E. Poodts, G. Minak, A. Zucchelli, Impact of sea-water on the quasi static and fatigue flexural properties of GFRP, Composite Structures. 97 (2013) 222–230. https://doi.org/10.1016/j.compstruct.2012.10.021.

[13] A. Boisseau, P. Davies, F. Thiebaud, Fatigue behaviour of glass fibre reinforced composites for ocean energy conversion systems, Applied Composite Materials. 20 (2013) 145–155. https://doi.org/10.1007/s10443-012-9260-0.

[14] N. Tual, N. Carrere, P. Davies, T. Bonnemains, E. Lolive, Characterization of sea water ageing effects on mechanical properties of carbon/epoxy composites for tidal turbine blades, Composites Part A: Applied Science and Manufacturing. 78 (2015) 380–389. https://doi.org/10.1016/j.compositesa.2015.08.035.

[15] C. Vosgien Lacombre, G. Bouvet, D. Trinh, S. Mallarino, S. Touzain, Water uptake in free films and coatings using the Brasher and Kingsbury equation: a possible explanation of the different values obtained by electrochemical Impedance spectroscopy and gravimetry, Electrochimica Acta. 231 (2017). https://doi.org/10.1016/j.electacta.2017.02.051.

[16] A. Chateauminois, L. Vincent, B. Chabert, J.P. Soulier, Study of the interfacial degradation of a glass-epoxy composite during hygrothermal ageing using water diffusion measurements and dynamic mechanical thermal analysis, Polymer (Guildf). 35 (1994) 4766–4774. https://doi.org/10.1016/0032-3861(94)90730-7.

[17] A. Fick, Ueber Diffusion, Ann Phys. (1855) 59–86.

[18] P. Davies, Y.D.S. Rajapakse Editors, Durability of Composites in a Marine Environment, n.d. https://doi.org/10.1007/978-94-007-7417-9.

[19] S. Popineau, C. Rondeau-mouro, C. Sulpice-gaillet, M.E.R. Shanahan, Free / bound water absorption in an epoxy adhesive, Polymer (Guildf). 46 (2005) 10733–10740. https://doi.org/10.1016/j.polymer.2005.09.008.

[20] H.G. Carter, K.G. Kibler, H.G. Carter, K.G. Kibler, Langmuir-Type Model for Anomalous Moisture Diffusion in Composite Resins, Journal of Composite Materials. 12 (1978) 118–131. https://doi.org/10.1177/002199837801200201.

[21] J. El, G. Lubineau, F. Roger, J. Verdu, A fully coupled diffusion-reaction scheme for moisture sorption e desorption in an anhydride-cured epoxy resin, Polymer (Guildf). 53 (2012) 5582–5595. https://doi.org/10.1016/j.polymer.2012.09.037.

[22] M. Gigliotti, F. Jacquemin, A. Vautrin, Assessment of approximate models to evaluate transient and cyclical hygrothermoelastic stress in composite plates, International Journal of Solids and Structures. 44 (2007) 733–759. https://doi.org/10.1016/j.ijsolstr.2006.05.014.

[23] M. Beringhier, A. Djato, D. Maida, M. Gigliotti, A novel protocol for rapid identification of anisotropic diffusion properties of polymer matrix composite materials with complex texture, Composite Structures. 201 (2018) 1088–1096. https://doi.org/10.1016/j.compstruct.2018.05.142.

[24] I.B.C.M. Rocha, S. Raijmaekers, F.P. Van Der Meer, R.P.L. Nijssen, H.R. Fischer, L.J. Sluys, Combined experimental / numerical investigation of directional moisture diffusion in glass / epoxy composites, Composites Science and Technology. 151 (2017) 16–24. https://doi.org/10.1016/j.compscitech.2017.08.002.

[25] P. Davies, P.Y. Le Gac, M. Le Gall, M. Arhant, Marine Ageing Behaviour of New Environmentally Friendly Composites, Solid Mechanics and Its Applications. 245 (2018) 225–237. https://doi.org/10.1007/978-3-319-65145-3_12.

[26] F.E. Fowle, The Spectroscopic Determination of Aqueous Vapor, The Astrophysical Journal. 35 (1912). https://doi.org/10.1086/141923.

[27] G. Korotcenkov, Handbook of Humidity Measurement Methods, Materials and Technologies Volume 3: Sensing Materials and Technologies, in: 2020: pp. 1–22.

[28] A.E. Krauklis, A.I. Gagani, A.T. Echtermeyer, Near-Infrared Spectroscopic Method for Monitoring Water Content in Epoxy Resins and Fiber-Reinforced Composites, Materials. 11 (2018). https://doi.org/10.3390/MA11040586.

[29] H. Va\vsková, A powerful tool for material identification: Raman spectroscopy, in: 2011.

[30] C. Marro Bellot, M. Olivero, M. Sangermano, M. Salvo, Towards self-diagnosis composites: Detection of moisture diffusion through epoxy by embedded evanescent wave optical fibre sensors, Polymer Testing. 71 (2018) 248–254. https://doi.org/10.1016/J.POLYMERTESTING.2018.09.019.

[31] G. Bouvet, D. Trinh, S. Mallarino, X. Feaugas, In situ monitoring of organic coating swelling by dynamic mechanical analysis and scanning electrochemical microscopy, Progress in Organic Coatings. 96 (2016) 13–18. https://doi.org/10.1016/j.porgcoat.2016.01.026.

[32] Y. Elkebir, S. Mallarino, D. Trinh, S. Touzain, Effect of physical ageing onto the water uptake in epoxy coatings, Electrochimica Acta. (2020). https://doi.org/10.1016/j.electacta.2020.135766.

[33] C. Vosgien Lacombre, G. Bouvet, S. Cohendoz, D. Trinh, X. Feaugas, S. Touzain, S. Mallarino, Influence of internal stresses on the physicochemical and mechanical properties evolution of pigmented epoxy systems during hygrothermal ageing, Surface and Coatings Technology. 341 (2018) 86–94. https://doi.org/10.1016/J.SURFCOAT.2017.10.013.

[34] M. Keddam, N. Portail, D. Trinh, V. Vivier, Progress in scanning electrochemical microscopy by coupling with electrochemical impedance and quartz crystal microbalance, ChemPhysChem. 10 (2009). https://doi.org/10.1002/cphc.200900506.

[35] D. Trinh, M. Keddam, X.R. Novoa, V. Vivier, Alternating-current measurements in scanning electrochemical microscopy, part 1: Principle and theory, ChemPhysChem. 12 (2011). https://doi.org/10.1002/cphc.201001084.

[36] C. Horwood, M. Stadermann, Evaluation of a Ag / Ag 2 S reference electrode with long-term stability for electrochemistry in ionic liquids, Electrochemistry Communications. 88 (2018) 105–108. https://doi.org/10.1016/j.elecom.2018.02.005.

[37] N. Bodappa, Y. Fu, P. Broekmann, J. Furrer, K. Zick, S. Vesztergom, H. Tahara, T. Sagara, Electron transfer controlled by solvent and counter-anion dynamics in electrochemistry of viologen-type ionic liquid, Electrochimica Acta. 320 (2019) 134559. https://doi.org/10.1016/j.electacta.2019.134559.

[38] D. Moulin, P.C. Howlett, D.R. Macfarlane, Electrochemistry of the tris (2,2‘-bipyridine) complex of iron (II) in ionic liquids and aprotic molecular solvents, Electrochimica Acta. 220 (2016) 347–353. https://doi.org/10.1016/j.electacta.2016.10.126.

[39] T.J. Stockmann, P.D. Boyle, Z. Ding, Preparation and crystal structure of tetraoctylphosphonium tetrakis (pentafluorophenyl) borate ionic liquid for electrochemistry at its interface with water, Catalysis Today. 295 (2017) 89–94. https://doi.org/10.1016/j.cattod.2017.05.030.

[40] D. Trinh, C. Vosgien-Lacombre, G. Bouvet, S. Mallarino, S. Touzain, Use of ionic liquids in SECM experiments to distinguish effects of temperature and water in organic coating swelling, Progress in Organic Coatings. 139 (2020). https://doi.org/10.1016/j.porgcoat.2019.105438.

[41] C.A. Nkuku, R.J. Lesuer, Electrochemistry in Deep Eutectic Solvents, Journal of Physical Chemistry B. 111 (2007) 13271–13277.

[42] D.A. Walsh, K.R.J. Lovelock, P. Licence, D.A. Walsh, Ultramicroelectrode voltammetry and scanning electrochemical microscopy in room-temperature ionic liquid electrolytes, Chemical Society Reviews. (2010) 4185–4194. https://doi.org/10.1039/b822846a.

[43] M. Echeverría, F.J. Deive, M.A. Sanromán, A. Rodríguez, C.M. Abreu, C.A. Echeverría, An Inert Ionic Liquid-Based System for Ascertaining Electrolyte Diffusivity in Protective Coatings, Corrosion. 71 (2015) 259–266. https://doi.org/10.5006/1362.

[44] C. Zhao, A.M. Bond, X. Lu, Determination of Water in Room Temperature Ionic Liquids by Cathodic Stripping Voltammetry at a Gold Electrode, Anal Chem. 84 (2012) 2784–2791.

[45] Q. Qian, P. Yu, H. Cheng, X. Wang, L. Yang, Electrochemical Quantification of Hygroscopicity of Ionic Liquids with Solution-Dissolved Potassium Ferricyanide as the Redox Probe, Electroanalysis. (2011) 2870–2877. https://doi.org/10.1002/elan.201100533.

[46] M.J.A. Shiddiky, A.A.J. Torriero, C. Zhao, I. Burgar, G. Kennedy, A.M. Bond, Nonadditivity of Faradaic Currents and Modification of Capacitance Currents in the Voltammetry of Mixtures of Ferrocene and the Cobaltocenium Cation in Protic and Aprotic Ionic Liquids, J Am Chem Soc. 131 (2009) 7976–7989.

[47] Q. Qian, P. Yu, H. Cheng, X. Wang, L. Yang, Electrochemical Quantification of Hygroscopicity of Ionic Liquids with Solution-Dissolved Potassium Ferricyanide as the Redox Probe, Electroanalysis. (2011) 2870–2877. https://doi.org/10.1002/elan.201100533.

[48] M. Hampel, M. Schenderlein, C. Schary, M. Dimper, O. Ozcan, Efficient detection of localized corrosion processes on stainless steel by means of scanning electrochemical microscopy (SECM) using a multi- electrode approach, Electrochemistry Communications. 101 (2019) 52–55. https://doi.org/10.1016/j.elecom.2019.02.019.

[49] L. Tian, X. Wang, L. Zhao, M. Shi, H. Wang, X. Zhang, Direct detection of label-free blood fingermarks by SECM imaging, Electrochemistry Communications. 102 (2019) 89–93. https://doi.org/10.1016/j.elecom.2019.04.003.

[50] M.B. Jensen, M.J. Peterson, N. Jadhav, V.J. Gelling, SECM investigation of corrosion inhibition by tungstate- and vanadate-doped polypyrrole/aluminum flake composite coatings on AA2024-T3 We dedicate this manuscript to our colleague, mentor, and friend, Professor Gordon P. Bierwagen., Progress in Organic Coatings. 77 (2014) 2116–2122. https://doi.org/10.1016/j.porgcoat.2014.05.019.

[51] J.A. Ramírez-cano, L. Veleva, R.M. Souto, B.M. Fernández-pérez, SECM study of the pH distribution over Cu samples treated with 2-mercaptobenzothiazole in NaCl solution, Electrochemistry Communications. 78 (2017) 60–63. https://doi.org/10.1016/j.elecom.2017.04.005.

[52] O. Fontaine, C. Lagrost, J. Ghilane, P. Martin, G. Trippé, C. Fave, J. Lacroix, P. Hapiot, H.N. Randriamahazaka, Mass transport and heterogeneous electron transfer of a ferrocene

derivative in a room-temperature ionic liquid, Journal of Electroanalytical Chemistry. 632 (2009) 88–96. https://doi.org/10.1016/j.jelechem.2009.04.001.

[53] C.A. Nkuku, R.J. Lesuer, Electrochemistry in Deep Eutectic Solvents, Journal of Physical Chemistry B. 111 (2007) 13271–13277.

[54] Y. Elkebir, S. Mallarino, D. Trinh, S. Touzain, Effect of physical ageing onto the water uptake in epoxy coatings, Electrochimica Acta. (2020). https://doi.org/10.1016/j.electacta.2020.135766.

[55] B.D.S. Silvester, R.G. Compton, Electrochemistry in Room Temperature Ionic Liquids : A Review and Some Possible Applications, Zeitschrift Für Physikalische Chemie. 220 (2006) 1247–1274. https://doi.org/10.1524/zpch.2006.220.10.1247.

[56] K.R.J. Lovelock, F.N. Cowling, A.W. Taylor, P. Licence, D.A. Walsh, Effect of Viscosity on Steady-State Voltammetry and Scanning Electrochemical Microscopy in Room Temperature Ionic Liquids, The Journal of Physical Chemistry B. 114 (2010) 4442–4450. https://doi.org/10.1021/jp912087n.

[57] O. Fontaine, C. Lagrost, J. Ghilane, P. Martin, G. Trippé, C. Fave, J. Lacroix, P. Hapiot, H.N. Randriamahazaka, Mass transport and heterogeneous electron transfer of a ferrocene derivative in a room-temperature ionic liquid, Journal of Electroanalytical Chemistry. 632 (2009) 88–96. https://doi.org/10.1016/j.jelechem.2009.04.001.

Water saturated resin

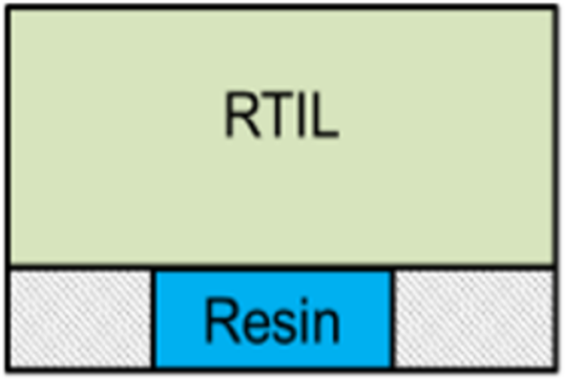

t = 0

Probing moisture gradient

SECM tip

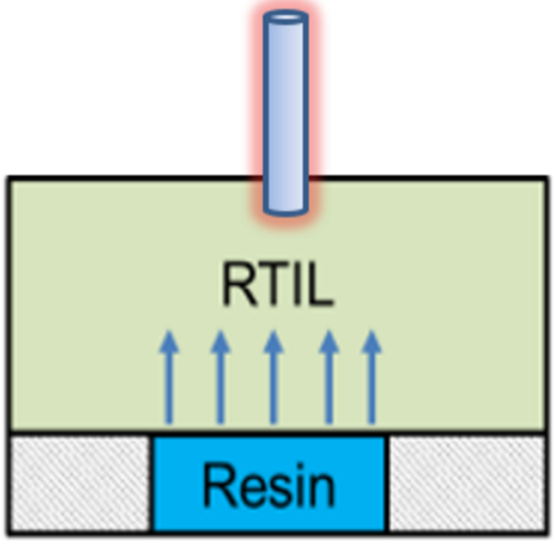

0 < t < 20 hours

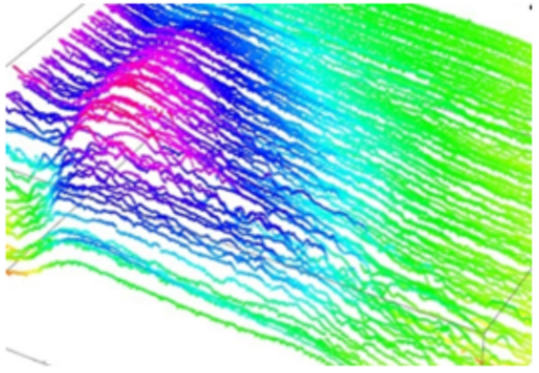

Observing water content coming from the resin